Published in final edited form as:
Dev Biol. 2007 September 15; 309(2): 306–316. doi:10.1016/j.ydbio.2007.07.019.

Combinations of *WOX* activities regulate tissue proliferation during *Arabidopsis* embryonic development

Xuelin Wu[1,4], **Joanne Chory**[1,2], and **Detlef Weigel**[1,3,*]

[1]Plant Biology Laboratory, The Salk Institute for Biological Studies, La Jolla, CA 92037, USA

[2]Howard Hughes Medical Institute, La Jolla, CA 92037, USA

[3]Department of Molecular Biology, Max Planck Institute for Developmental Biology, D-72076 Tübingen, Germany

Abstract

Tissue growth as the result of cell division is an essential part of embryonic development. Previous studies have shown that STIMPY (STIP)/WOX9, a homeodomain transcription factor of the *Arabidopsis thaliana* WOX family, is required for maintaining cell division and preventing premature differentiation in emerging seedlings. Here we present evidence that *STIP* performs similar functions during embryogenesis. Complete loss of *STIP* activity results in early embryonic arrest, most likely due to a failure in cell division. *STIMPY-LIKE* (*STPL*)/*WOX8*, a close homolog of *STIP* in *Arabidopsis*, also positively regulates early embryonic growth, and can replace *STIP* function when expressed under the *STIP* promoter. *STPL* shares redundant functions with a more distantly related member of the *WOX* family, *WOX2*, in regulating embryonic apical patterning. These findings show that combinatorial action of WOX transcription factors is essential for *Arabidopsis* embryonic development.

Keywords

Arabidopsis; homeodomain; pattern formation; WUSCHEL; WOX genes; STIMPY; genetic redundancy

Introduction

Embryogenesis transitions a single-cell zygote to a multi-cellular individual. Compared to that of higher animals, the mature embryo of higher plants is of relatively simple structure. It displays basic body polarities and contains the primary shoot and root meristems, which are the origins of post-embryonic growth. As in all multi-cellular organisms, this transformation is accomplished by the close coordination between two major processes: pattern formation and cell fate determination on one hand, and cell proliferation and tissue growth on the other.

* Mailing address of corresponding author: Detlef Weigel, Dept. of Molecular Biology, MPI for Developmental Biology, Spemannstrasse 37-39/VI, D-72076 Tübingen, Germany, EM: weigel@weigelworld.org, PH: +49-7071-601-1411, FX: +49-70710601-1412.

[4]Current address: Molecular and Computational Biology, University of Southern California, Los Angeles, CA 90089-2910

Embryonic patterning events in *Arabidopsis* have been the topic of extensive studies in the past two decades. Two major axes are established at early stages of embryonic development, the apical-basal and the radial axes (reviewed in Jürgens, 2003; Laux et al., 2004; Willemsen and Scheres, 2004). Genetic and molecular analyses have identified the plant hormone auxin as a prominent player along the apical-basal axis (recently reviewed by Jenik and Barton, 2005; Weijers and Jürgens, 2005). More recently, a number of other molecules and mechanisms have been implicated in the correct establishment of apical-basal polarity in *Arabidopsis* embryos. Some examples include the MAP kinase pathway as revealed by the function of *YODA* (Lukowitz et al., 2004), or transcriptional repression as inferred from the activities of the *TOPLESS* gene and histone acetyltransferases (Long et al., 2006; Long et al., 2002). As the embryo passes from the globular stage to the heart stage, it acquires bilateral symmetry through the formation of the cotyledon primordia. Interactions among the auxin response genes, the *CUP-SHAPED COTYLEDON* (*CUC1-3*) genes (Aida et al., 1997; Vroemen et al., 2003), and other genetic pathways specify the cotyledon boundaries by restricting cell proliferation between the primordia, and allow the formation of the shoot apical meristem (Aida et al., 1999; Aida et al., 2002; Barton and Poethig, 1993; Bennett et al., 1995; Berleth and Jürgens, 1993; Friml et al., 2003).

A continuous process underlying the patterning events of embryogenesis is cell proliferation, without which the embryo fails to increase in size. The finely tuned balance of cell division vs. differentiation decisions is especially important for plant embryos in controlling both size and shape, since cells cannot migrate. Mutations in genes such as *FASS*/*TONNEAU2* (Camilleri et al., 2002; Mayer et al., 1991; Torres-Ruiz and Jürgens, 1994) and *RASSPBERRY*1-3 (Apuya et al., 2002; Yadegari et al., 1994) lead to partial uncoupling of division and differentiation, resulting in severe embryonic defects. Much progress has been made in understanding plant cell cycle regulation in recent years, and many genes directly involved in the cell cycle machinery have been identified (reviewed by Inzé and De Veylder, 2006). It has been shown that mutations in some of the cell cycle genes cause embryonic developmental defects (e.g., Blilou et al., 2002; Willemsen et al., 1998). However, how tissue proliferation is regulated in a developmental context during embryogenesis remains poorly understood.

Recently, Haecker and colleagues described a group of homeobox transcription factors in *Arabidopsis* that share similarity with *WUSCHEL* (*WUS*, Laux et al., 1996), which they named the *WUSCHEL-RELATED HOMEOBOX* (*WOX*) genes (Haecker et al., 2004). An outlying clade of the *WOX* group contains *STIMPY* (*STIP*/*WOX9*) and its paralog *WOX8*, which we named *STIMPY-LIKE* (*STPL*), reflecting its high similarity to *STIP* (Haecker et al., 2004; Wu et al., 2005). *STIP* promotes cell proliferation and prevents premature differentiation in meristematic tissues during post-embryonic development (Wu et al., 2005). Here we show that *STIP* is also essential for maintaining tissue growth during embryogenesis. *STPL*, on the other hand, plays a minor role and acts partially redundantly with *STIP* in promoting proliferation. We present evidence that *STPL* acts redundantly with another member of the *WOX* group, *WOX2*, in regulating cotyledon separation. Recently, it has been reported that, similar to the function of *WUS* in the shoot meristem, *WOX5* is involved in the maintenance of the stem cells in the root (Sarkar et al., 2007). Together with our results, these findings suggest that combinations of WOX activities regulate different aspects of tissue proliferation in *Arabidopsis* embryonic development.

Materials and Methods

Plant material

Plants were grown in long days (16 hours light/8 hours darkness) under about 120 μE m^{-2} sec^{-1} light provided by a 3:1 mixture of cool-white and GroLux (Osram Sylvania)

fluorescent bulbs, at 23°C. To observe seedling phenotypes, seeds were germinated on 1/2 Murashige Minimal Organics Medium (GIBCO) with 0.6% agar. The plates were moved to 23°C after two days of stratification at 4°C.

stip-1 and *stip*-2 have been described (Wu et al., 2005). *stip*-3 was an EMS mutant allele identified in a Tilling screen (Till et al., 2003). It contains a G to A change at nucleotide position 14349811 of Chromosome 2, resulting in a non-sense mutation of codon 261. It was originally generated in Columbia *erecta* background, and was backcrossed to Columbia-0 for five generations before phenotypic analysis.

All other T-DNA insertions lines used in this study were identified from the Salk T-DNA collection, and are in the Columbia ecotype (Alonso et al., 2003). The annotated T-DNA insertion sites were confirmed as correct by sequencing in all lines except Salk_114607, which was found to carry a T-DNA insertion at nucleotide position 23951085 of chromosome 5, approximately 250 bp upstream of the annotated insertion site. T-DNA lines were genotyped with the T-DNA border primer LBb1 (http://signal.salk.edu/) in combination with the following gene-specific primers:

Salk_014799 5′-gaaatcgatactccatcttacatgcac-3′ & 5′-aatggaacagtcaaaggaggaaaac-3′;

Salk_114607 5′-ccttgctcaaacggcacgtag-3′ & 5′-ccattactatcgaaacgagtagaagtag-3′;

Salk_004777 5′-ggttgaaacccacccagaattg-3′ & 5′-cagcttaccacatcatagtggg-3′;

Salk_033323 5′-cgtcaaggattcatcatcaggtacg-3′ & 5′-cgcaggatctaattcatgctaagc-3′;

Salk_087882 5′-gctttacggattgatgcagctc-3′ & 5′-caatcgaccgtatatgttcccac-3′.

Salk_014799 has an insertion in the second exon of *STPL* (At5g45980) and no full-length mRNA can be detected using RT-PCR. Therefore it is considered a null allele. Salk_114607 has an insertion in the second exon of *WOX2* (At5g59340); Salk_033323 has an insertion in the second exon of *WOX6* (at2g01500); Salk_087882 has an insertion in the second intron of *WOX12* (At5g17810). In all three cases, no transcript spanning the insertion sites was detected in plants homozygous for the insertion, using RT-PCR. Salk_004777 has an insertion in the second exon of *WOX11* (At3g03660). We could not detect *WOX11* transcript with RT-PCR in any of the tissue types tested, although the location of the insertion suggests that it should be a strong hypomorphic allele. For double mutant analysis, all crosses were followed to F3 or F4 generations to confirm the genotype and phenotype of the progeny.

Plasmid construction

The STIP-GFP fusion was created by inserting the GFP coding sequence at the C-terminus of the 8.1 kb *STIP* genomic sequence, right in front of the stop codon. It includes the 5.6 kb *STIP* promoter (Wu et al., 2005) and 450 bp of its 3′ UTR region. For expressing *STPL* under the control of *STIP* promoter, the 5.6 kb *STIP* promoter fragment was linked to a 2 kb genomic fragment of *STPL*, which include 65 bp of *STPL* 5′ UTR and 180 bp of 3′ UTR. Both were shuttled into the binary vector pMX202 (Wu et al., 2003) and transformed into *stip*-2/+ plants. Plant transformation was carried out using the floral dip method (Weigel and Glazebrook, 2002). Transgenic seedlings were selected on MS agar plates containing 50 μg/ml kanamycin, then transplanted to soil. At least 50 T1 lines were generated and analyzed for each transgene.

Histological Analysis

In situ hybridization was performed as described (Wu et al., 2005). GUS staining was done as described (Sessions et al., 1999), using 2 mM potassium ferro and ferri cyanide, at 37°C

for 12 to 14 hours. The GUS-stained ovules were cleared with 30% glycerol containing 2.5 g/ml chloral hydrate.

For morphological studies of mutant embryos, ovules were removed from young siliques and cleared in 30% glycerol containing 2.5 g/ml chloral hydrate. Mature embryos were removed from the seed coat without clearing.

Tissue sections, GUS-stained samples, and cleared ovules were photographed on a Leica DM5000B compound microscope equipped with a SPOT camera. All comparative samples were taken under identical magnifications. Seedlings samples were photographed using a Leica MZFLIII dissecting microscope with a DC300F camera. GFP fluorescence was imaged with a Leica SPII AOBS confocal microscope.

Quantitative RT-PCR

Total RNA was extracted from the inflorescences, open flowers, and green siliques of soil-grown Col-0 wild type, *stip*-1, and *stpl*-1 plants using the Spectrum Plant RNA kit (Sigma). First-strand cDNA was synthesized using Superscript III First-Strand cDNA Synthesis kit (Invitrogen). Quantitative PCR reactions were done using the SYBR Green method in a BioRad iCycler in duplicates, and data was analyzed using BioRad MyiQ Single-Color Real-Time PCR Detection System. *UBQ-10* served for normalization. The primers used for each gene are as follows:

STIP (At2g33880): 5′-ccatcaacttcggaccagctt-3′ and 5′-tccctcacattgaacggtcct-3′;

STPL (At5g45980): 5′-atggaaatggcggtggaaa-3′ and 5′-acaccgtcattctcaccggat-3′;

UBQ-10 (At5g15400): 5′-tgcgctgccagataatacactatt-3′ and 5′-tgctgcccaacatcaggtt-3′.

Flow cytometry

Nuclei were isolated from roots of vertical agar-grown 7-day-old Col-0 and *stip*-1 seedlings using methods previously described (Dolezel and Gohde, 1995), with the exception that nuclei were stained with SYBR Green (1:10,000; Molecular Probes). Nuclei were also isolated from imbibed seeds to be used as the diploid control (Masubelele et al., 2005). 20,000 nuclei for each sample were sorted using a FACScan system (Becton-Dickinson), and data were analyzed using FlowJo.

Results

STIP is expressed in growing embryos

In *Arabidopsis thaliana*, embryogenesis begins with an asymmetric division of the elongated zygote into a smaller apical cell and a larger basal cell. The basal cell undergoes limited divisions to generate the suspensor, which connects the developing embryo to the maternal tissue; the upper-most daughter cell derived from the basal cell is the hypophysis, which becomes the basal-most region of the embryo. The apical daughter cell, in the meantime, enters a highly regular cell division pattern to form the embryo proper, which goes through the globular, the heart, and the torpedo stages before reaching its final form (Mansfield and Briarty, 1991).

Previously we have found that *STIP* is expressed in young proliferating tissues during post-embryonic development (Wu et al., 2005). Since it was originally named after its loss-of-function embryonic phenotypes, we set out to determine *STIP* expression pattern during embryonic development. Using *in situ* hybridization, we first detected *STIP* mRNA in the zygote after the first cell division post fertilization, in both the apical and the basal cells (Figure 1A). As both the embryo proper and the suspensor continue to divide, *STIP*

expression in the embryo proper and the hypophysis becomes stronger than that of the suspensor (Figure 1B, C). By the late globular stage, it is expressed uniformly throughout the embryo (Figure 1D). As the embryos start to elongate and form the cotyledons, *STIP* expression becomes more concentrated in the cotyledon primordia and the outer cell layers in basal half of the embryo, and starts to clear from the central portion of the embryo (Figure 1E). This pattern persists through the torpedo stage (Figure 1F), until expression subsides when the embryo is near maturity (data not shown).

Since the *STIP* mRNA pattern detected by us is broader than what was reported by Haecker and colleagues (2004), we further examined the STIP protein expression pattern using a STIP-GFP fusion protein expressed from the endogenous *STIP* promoter. When this transgene was transformed into the *stip*-2 background, it was able to fully rescue both the embryonic and post-embryonic defects of homozygous *stip*-2 plants, suggesting that the fusion protein is functional and that its expression domain resembles the endogenous STIP protein pattern.

When we examined the STIP:GFP fusion in embryos derived from rescued *stip*-2 plants, we found that it is expressed in low levels in a pattern consistent with our *in situ* hybridization results. GFP fluorescence could be detected as early as the first zygotic division in both the apical and the basal daughter cells, and is both nuclear and cytoplasmic (Figure 1G). The nuclear portion becomes more pronounced as cell divisions progress in both the suspensor and the embryo. Unlike what was seen in *STIP* mRNA expression, the STIP:GFP signal in the suspensor cells at early globular stage appears much stronger than that of the embryos (Figure 1H). This discrepancy may be due to the vacuolation of the suspensor cells, which pushes the cytoplasm close to the cell wall, making the detection of mRNA difficult. By late globular to early transition stage, the STIP:GFP fusion protein is evenly distributed through out the embryo and the suspensor (Figure 1I). The basal half of the embryo, especially cells in the protoderm layer, starts to show slightly higher levels of expression by early heart stage (Figure 1J). Unfortunately, we were not able to image embryos beyond early heart stage due to the combination of low expression levels of the fusion protein and auto-fluorescence interference.

Complete loss of *STIP* function results in early embryonic arrest

To understand *STIP*'s role in embryogenesis, we examined the phenotype of embryos derived from plants heterozygous for three *STIP* loss-of-function alleles: *stip*-1, a hypomorphic allele resulted from a transposon insertion in the second intron, and the namesake of *STIP*; *stip*-2, which carries a stop codon within the homeobox; and *stip*-3, which contains a non-sense mutation after the homeobox. We found that the three alleles lead to different degrees of embryonic lethality.

Of the three alleles, *stip*-1 displays the weakest phenotype (Figure 2 and Table 1). It only becomes apparent by early torpedo stage that approximately 25% (n=237) of the embryos from *stip*-1/+ plants fail to elongate along the apical-basal axis, and cells begin expanding horizontally instead (Figure 2B, compare to A). By the time the fruits reach maturity, only a very small portion of the embryos show lethality, another 30% show various degrees of reduction in size (Table 1). The majority of these seeds does germinate and can develop into full-size plants after being rescued by exogenous sugar (Wu et al., 2005), indicating that the reduction in size is not detrimental.

In comparison, embryonic defects can be clearly observed in 20% (n=174) of the progeny of *stip*-2/+ plants by early globular stage. While normal embryos undergo organized cell division and continue to grow (Figure 2C), the mutant embryos often arrest after the first few divisions (Figure 2D, E), with some showing abnormal division plane (Figure 2D). This

phenotype persists till fruit maturity, when about one quarter of the seeds contain embryos arrested at the globular stage or earlier (Table 1). A small percentage of the *stip*-2 homozygous embryos can reach seed maturity and germinate (Wu et al., 2005).

stip-3 is the strongest allele included in this study. 28% (n=251) of the embryos from *stip*-3/+ plants, presumably homozygous for *stip*-3, show arrest within the first two to three divisions (Figure 2G, H, compare to F). Abnormal division patterns are sometimes seen in the suspensor region (Figure 2H). This growth arrest persists until seed maturation. Some additional seeds, most likely *stip*-3/+, also display reduced embryo size (Table 1). No seedling homozygous for *stip*-3 was ever recovered.

stip embryos show cell cycle arrest

The early lethality of *stip*-2 and *stip*-3 embryos poses problems for investigating the cause of the *stip* embryonic phenotype. Therefore, we turned to *stip*-1, which can often develop till maturation (Figure 3D, compare to A). In our previous study, we have shown that *stip*-1 embryos have reduced shoot meristem and apical-basal growth, but show correct root cap and root meristem gene expression (Wu et al., 2005). To exclude other patterning defects, we further examined the radial patterning in *stip*-1 embryos using *SCARECROW* (*SCR*), which marks the endodermal layer in the embryonic root and hypocotyl (Di Laurenzio et al., 1996). Normal distribution of SCR::GFP was seen in *stip*-1 embryos (Figure 3E, compare to B), confirming the earlier conclusion that the *stip*-1 phenotype is not due to patterning defects. Another possible cause of the *stip* phenotype is changes in auxin localization. When we examined auxin localization using the DR5rev::GFP transgene (Friml et al., 2003), we found normal DR5 pattern at the tip of the cotyledons and in the hypophysis in *stip*-1 embryos (Figure 3F, compare to C), suggesting that the reduced growth is not caused by disruption in auxin localization.

Our earlier study had shown that the post-embryonic growth arrest seen in surviving *stip*-1 and *stip*-2 seedlings is associated with cell division arrest. We therefore examined cell division patterns in *stip*-2 embryos using *CDKA*;1 (previously called *CDC2A*; Joubes et al., 2000) expression. It has been demonstrated that *CDKA;1* is expressed throughout the cell cycle in *Arabidopsis*, and the expression pattern of a β-glucuronidase (GUS) reporter driven by the *CDKA;1* promoter mimics endogenous *CDKA;1* gene expression (Beeckman et al., 2001; Hemerly et al., 1993; Martinez et al., 1992). Among the embryos collected from *stip*-2/+ plants carrying the *CDKA;1* reporter, high GUS activity was detected throughout the heart stage embryos of normal morphology, presumed to be homozygous or heterozygous for the wild-type allele (Figure 4A). In comparison, GUS activity was much reduced or even absent in mutant embryos, which had delayed development or had entered complete growth arrest (Figure 4B, C). This observation indicates that similar to the post-embryonic effects, *STIP* is required for maintaining cell division in growing embryos.

A natural question to ask in the case of cell division arrest is where in the cell cycle it occurs. Since it is very difficult to isolate embryonic tissue without maternal contamination, we took advantage of the similarity between embryonic and post-embryonic *stip* phenotypes. Root nuclei were isolated from wild-type and growth-arrested *stip*-1 seedlings and their DNA content was determined by flow cytometry. As shown in Table 3 and Figure 4D, there is a significant increase in the percentage of 4C nuclei in *stip*-1 compared to the wild-type sample. This suggests that *stip* mutant cells are likely to arrest in the G2 phase.

STPL acts partially redundantly with *STIP* in promoting embryonic cell division

STIP and STPL share 41% overall identity at the protein level, with nearly identical homeodomains and high similarity in the C-terminal region. To test whether STPL and STIP

proteins also have similar activities, we expressed *STPL* under the control of the *STIP* promoter in *stip*-2 background. Among the 83 T1 transgenic lines derived from *stip*-2/+ parents, 46 were heterozygous and 17 were homozygous for *stip*-2. Since the near Mendelian distribution was never seen in *stip*-2/+ progeny without the transgene, we conclude that this transgene is able to replace the function of *STIP* during embryonic development. 12 of the 17 *stip*-2 homozygous lines carrying the *STIP*::*STPL* transgene were completely rescued to fertile plants, suggesting that STPL protein can carry out the same functions as STIP.

To address the role of the *STPL* gene, we identified a T-DNA insertion allele of *STPL*, *stpl*-1, in the Salk T-DNA collection (Alonso et al., 2003). The T-DNA was inserted in the second exon, and no full-length *STPL* transcript could be detected in plants homozygous for *stpl*-1. Therefore it is presumably a null allele. In contrast to *stip* mutants, *stpl*-1 plants showed no phenotypic defect throughout the entire life cycle (data not shown). One possible reason for the lack of visible phenotypes in *stpl*-1, based on the finding that STPL can functionally replace STIP, is that *STIP* was up-regulated in *stpl*-1 plants, therefore compensating for the loss of *STPL*. To investigate this possibility, we compared *STIP* and *STPL* expression levels in wild-type, *stip*-1, and *stpl*-1 inflorescences, open flowers, and young siliques using quantitative RT-PCR (qRT-PCR). No significant change in *STIP* expression levels was detected (Table 2). Similarly we did not detect a change in *STPL* expression in *stip*-1 tissues (data not shown). These results make cross-regulation between *STIP* and *STPL* at the transcriptional level unlikely.

Another explanation for the lack of phenotype in *stlp*-1 plants is that *STPL* acts redundantly with other genes, and the best candidate for this redundancy is *STIP*. If this is the case, removing *STPL* from *stip* mutants might enhance the *stip* phenotype, and this is indeed what we found. We again chose *stip*-1 for this experiment for its milder phenotype. While *stpl*-1 embryos appear normal, and the majority of the *stip*-1 embryos can develop to maturity, approximately 25% (n=215) of embryos from *stpl*-1/*stpl*-1 *stip*-1/+ plants (presumably the *stip*-1 *stpl*-1 double mutants) show cell division defects as early as the first division in embryo proper (Figure 5B, C, compare to A). These embryos either stop growing completely after the first division, or enter a short period of disorganized cell division as seen in many early embryonic lethal mutants. DR5rev::GFP fluorescence was detected evenly in both the suspensor and the embryo proper of the arrested putative *stip*-1 *stpl*-1 double mutant embryos (Figure 5E, compare to D), which resembles the normal auxin response pattern immediately after the first zygotic division (Friml et al., 2003). This again suggests that the development of putative *stip*-1 *stpl*-1 embryos is disrupted as early as the first cell division in the embryo proper. The early arrest seen in these presumed *stip*-1 *stpl*-1 double mutant embryos was not corrected during later stages of development (Table 1), and no double mutant seedling was ever found during our study.

STPL acts redundantly with *WOX2* in embryonic apical patterning

The functional overlap between *STIP* and *STPL* led us to further test possible interactions between them and other members of the *WOX* group genes. Based on the protein sequence similarity of the homeodomains, the closest relatives of *STIP* and *STPL* in the *Arabidopsis* genome are *WOX11* and *WOX12* (Haecker et al., 2004). We obtained T-DNA insertion lines for both genes. In both cases, plants homozygous for the insertion lack an apparent phenotype. Other than the interaction between *STIP* and *STPL*, no additional genetic interaction was observed in double mutant combinations among *STIP*, *STPL*, *WOX11*, and *WOX12*.

Two other *WOX* genes less closely related to *STIP* and *STPL* also caught our attention. *WOX2* appeared interesting, because it has been reported to be required for correct early

embryonic divisions, although the phenotype was corrected at later stages of embryogenesis (Haecker et al., 2004). Closely related to *WOX2* is *WOX6* (also called *PFS2* and *HOS9*; Park et al., 2005; Zhu et al., 2004), which shares significant homology with *WOX2* in the homeodomain. The inactivation of *WOX6* causes reduced fertility due to ovule defects (Park et al., 2005), which is also a phenotype observed in surviving *stip* mutant plants (Wu et al., 2005). When we generated double mutant combinations among *stip*, *stpl*, *wox2*, and *wox6*, we observed no phenotypic enhancement in *stip*-1 *wox6*, *stpl*-1 *wox6*, *wox2 wox6*, and *stip*-1 *wox2* double mutants. Surprisingly, although both *stpl*-1 and *wox2* mutant seedlings are fully viable and exhibit no visible defect, 32% of the *stpl*-1 *wox2* double mutant seedlings show different degrees of cotyledon defects, including asymmetric cotyledons and partial cotyledon fusion. These seedlings often also have only one of the first pair of true leaves (Figure 6B, C, D). All *stpl*-1 *wox2* plants show normal post-embryonic development. Therefore, *STPL* and *WOX2* are required for embryonic apical patterning.

Discussion

Plants control the size and shape of their organs via two approaches: cell division and cell expansion upon differentiation. During embryogenesis, embryos increase in size predominantly by cell division, transforming a single-cell zygote into a mature embryo. We have shown that *STIP* is required for maintaining cell division in both the embryo and the suspensor in *Arabidopsis*. Compared to *STIP*, *STPL* plays a relatively minor role in this process, which can only be seen when STIP activity is compromised. Interestingly, *STPL* also carries out redundant functions with *WOX2* in promoting cotyledon separation.

STIP is a key regulator of embryonic growth

We have previously reported that *STIP* is required for maintaining cell division in postembryonic proliferating tissues (Wu et al., 2005). Here, we extend the study to the embryonic stage. Our results show that *STIP* is expressed in the growing embryo and is required for the maintenance of cell division. After the heart stage, *STIP* expression is much reduced in the central portion of the embryo (Figure 1F). This is reminiscent of the changes that occur in the embryonic histone H4 expression pattern (data not shown), which marks the actively dividing cells. This similarity implies that *STIP* is only required during the proliferation phase. The alterative hypothesis, that STIP is a repressor of cell cycle exit/differentiation, seems unlikely because the lack of *CDKA;1* reporter activity in *stip*-2 mutant embryos (Figure 4A) indicates an absence of dividing cells (Beeckman et al., 2001; Hemerly et al., 1993; Martinez et al., 1992). Furthermore, we have previously found that *stip* mutant seedlings show premature differentiation of all meristematic tissues (Wu et al., 2005). Finally, mutant studies have suggested that the uncoupling of proliferation and differentiation during *Arabidopsis* embryogenesis is more likely to result in deformed embryos such as the *raspberry* mutants (Apuya et al., 2002; Yadegari et al., 1994).

While the weaker *stip* alleles show defects only in the embryo, the phenotype of *stip*-3 suggests that it is also involved in regulating cell division in the suspensor (Figure 2H). This is consistent with our observation that *STIP* is expressed in both the embryo and the suspensor (Figure 1). Therefore, *STIP* is essential for embryonic growth. The limited cell divisions that can occur in a strong *stip* embryo are possibly due to residual maternal contribution of cell cycle promoting factors.

The three *stip* alleles show different degrees of embryonic defects, with *stip*-2 having a nonsense mutation that is 5′ towards the *stip*-3 nonsense mutation. Intriguingly, *stip*-3, which is predicted to leave the homeodomain largely intact, has a stronger phenotype than *stip*-2, which is predicted to encode a protein lacking most of the homeodomain. Since protein-protein interactions often lie outside the homeodomain, it is possible that the strong

defects seen in *stip*-3 are due to dominant-negative effects caused by the truncated stip-3 protein. Further analysis is required to further dissect the biochemical activity of the mutant protein.

Auxin localization as the result of polar transport plays an important role in directing the establishment of the apical-basal axis and cotyledon outgrowth in the *Arabidopsis* embryo (Friml et al., 2003; Mayer et al., 1991; Shevell et al., 1994; Steinmann et al., 1999). However, we do not think that the *stip* phenotype is the result of changes in auxin response for several reasons. First, DR5rev::GFP localization and expression levels are not affected in *stip*-1 mutant embryos (Figure 3F), suggesting that the reduced growth seen in these embryos is not due to changes in auxin distribution. Secondly, *stip*-1 embryos form normal root meristem and cotyledons (Wu et al., 2005), both of which are often disrupted in auxin response mutants (Hamann et al., 1999; Mayer et al., 1991). Finally, strong *stip* embryos arrest growth as early as the first few cell divisions. This phenotype is far more severe than that of the auxin response mutants. This, taken together with our observation that *stip*-1 mutant embryos show normal patterning (Figure 3E, Wu et al., 2005), suggests that *STIP* functions in a novel pathway to promote cell division during *Arabidopsis* embryogenesis.

STPL functions redundantly with *STIP* in promoting cell division

STPL is highly similar in sequence to STIP. STPL is able to maintain cell division activity when expressed under the *STIP* promoter, demonstrating that the two proteins can carry out similar functions. Although the complete loss of *STPL* function alone causes no visible defect, further removal of *STPL* from the *stip*-1 background greatly enhances the *stip*-1 embryonic phenotype and leads to growth arrest as early as the first zygotic division. This indicates that *STPL* normally functions in promoting proliferation starting immediately after fertilization, but that it plays a minor role relatively, which only becomes apparent when STIP activity is compromised. Similar cases of unequal redundancy have been reported for other gene pairs in *Arabidopsis*, and the differences in gene functionality can be attributed to difference in expression levels or cross-regulation at the transcriptional and protein activity levels (reviewed by Briggs et al., 2006). While our results show that *STIP* and *STPL* mRNA levels do not change in response to the loss of the redundant homolog, we cannot exclude post-transcriptional cross-regulation. We have found that *STPL* is consistently expressed at a lower level than *STIP* in several tissues types, but the reasons behind this unequal redundancy of *STIP* and *STPL* remain to be investigated.

STPL and *WOX2* share redundant functions in embryonic apical patterning

In addition to the functional overlap with *STIP*, *STPL* also acts redundantly with *WOX2* in promoting cotyledon separation. During *Arabidopsis* embryogenesis, two separate cotyledons form by differential growth between the cotyledon primordia and the boundary region. A number of genes, including ones from the auxin response pathway, the *CUC* genes and other transcription factors, have been shown to be required in this process (Aida et al., 1997; Aida et al., 1999; Aida et al., 2002; Chandler et al., 2007; Prigge et al., 2005). Two classes of phenotypes are found in the mutants with cotyledon fusion: the ones with intact bilateral symmetry such as the *cuc* and *stm* mutants, and the ones with disrupted bilateral symmetry as seen in mutations affecting the auxin pathway (Aida et al., 2002). The *stpl wox2* double mutants sometime show disruption in bilateral symmetry with unequal cotyledons (Figure 6B), suggesting possible defects in auxin response. However, since genetic interactions have been reported among genes involved in the cotyledon separation process (Aida et al., 2002; Chandler et al., 2007), further analysis is needed to determine the precise function of *STPL* and *WOX2*.

Many genes required for proper cotyledon separation are also involved in the formation of the primary shoot apical meristem (Aida et al., 1997; Aida et al., 1999; Aida et al., 2002), although the two processes can be carried out independently (Vroemen et al., 2003). The *stpl wox2* double mutants, including the ones with a single cotyledon, develop fully functional shoot apical meristems (Figure 6D) and show no post-embryonic defect. This phenotype implies that *STPL* and *WOX2* may not be involved in shoot meristem formation. However, the variability and incomplete penetrance of phenotypic defects in *stpl wox2* double mutants strongly suggest the existence of additional degrees of functional redundancy.

Combinatorial *WOX* activities regulate tissue proliferation

STIP, *STPL*, and *WOX2* are all involved in regulating cell proliferation in the developing embryos. While *STIP* is essential in maintaining cell division throughout the embryo, *WOX2* appears to be involved in restricting proliferation at the cotyledon boundary. *STPL* has overlapping functions with both *STIP* and *WOX2*. Interestingly, this is not a simple case of functional redundancy among closely related genes. Depending on the genetic interaction partner, *STPL* can have opposite effects on proliferation: promoting cell division in early embryos along with *STIP*, and restricting proliferation at the cotyledon boundary when working together with *WOX2*. Furthermore, in contrast to the unequal redundancy between *STIP* and *STPL*, *STPL* and *WOX2* appear to share equal roles in a classic case of gene redundancy. In addition, since we did not observe redundant functions between *STPL* and *WOX11*, *WOX12*, which share much higher level of homology with *STPL* than *WOX2* (Haecker et al., 2004), the functional overlap between the *WOX* genes cannot simply be predicted by sequence homology.

Another *WOX* gene that is known to regulate proliferation is *WUS*, which is required for the establishment of the stem cell population in the embryonic shoot meristem (Laux et al., 1996). In our previous study, we have found that *stip*-1 embryos have reduced *WUS* expression and contain a smaller stem cell cluster within the shoot meristem, placing *STIP* genetically upstream of *WUS* (Wu et al., 2005). More recently, it has been reported that *WOX5* prevents premature differentiation of the stem cells in the root meristem. Furthermore, *WUS* and *WOX5* are functionally interchangeable in their ability to regulate stem cell proliferation (Sarkar et al., 2007). Similar to the case of *WOX2*/*STPL* redundancy, *WUS* is not the gene with the highest sequence similarity to *WOX5* in *Arabidopsis* (Haecker et al., 2004). Therefore, it may be a general feature of the *WOX* family that functional redundancy is not solely determined by overall protein sequence similarity. When we take all these cases into consideration, a picture of complex genetic interactions among this group of homeodomain transcription factors starts to emerge. Additional genetic and molecular analyses are needed to fully understand their role in regulating *Arabidopsis* embryonic development.

Acknowledgments

We thank Jeff Long, Dirk Inzé, and Jiří Friml for gifts of material; the University of Wisconsin (Madison) *Arabidopsis* Knock-out Facility, the *Arabidopsis* Tilling Project, and the Salk Institute Genome Analysis Laboratory for supplying T-DNA knock-out lines and tilling mutants; David Chambers and Katerina Bisova for help with the flow cytometry experiment; and Meng Chen and Sigal Savaldi-Goldstein for critical reading of the manuscript. This work was supported by a grant from NIH (GM62932) to J.C. and D.W., and a fellowship from the Life Sciences Research Foundation/U.S. Department of Energy to X.W. J.C. is an investigator of the Howard Hughes Medical Institute, and D.W. is a Director of the Max Planck Institute.

References

Aida M, Ishida T, Fukaki H, Fujisawa H, Tasaka M. Genes involved in organ separation in Arabidopsis: an analysis of the cup-shaped cotyledon mutant. Plant Cell 1997;9:841–57. [PubMed: 9212461]

Aida M, Ishida T, Tasaka M. Shoot apical meristem and cotyledon formation during *Arabidopsis* embryogenesis: interaction among the *CUP-SHAPED COTYLEDON* and *SHOOT MERISTEMLESS* genes. Development 1999;126:1563–70. [PubMed: 10079219]

Aida M, Vernoux T, Furutani M, Traas J, Tasaka M. Roles of *PIN-FORMED1* and *MONOPTEROS* in pattern formation of the apical region of the *Arabidopsis* embryo. Development 2002;129:3965–74. [PubMed: 12163400]

Alonso JM, Stepanova AN, Leisse TJ, Kim CJ, Chen H, Shinn P, Stevenson DK, Zimmerman J, Barajas P, Cheuk R, Gadrinab C, Heller C, Jeske A, Koesema E, Meyers CC, Parker H, Prednis L, Ansari Y, Choy N, Deen H, Geralt M, Hazari N, Hom E, Karnes M, Mulholland C, Ndubaku R, Schmidt I, Guzman P, Aguilar-Henonin L, Schmid M, Weigel D, Carter DE, Marchand T, Risseeuw E, Brogden D, Zeko A, Crosby WL, Berry CC, Ecker JR. Genome-wide insertional mutagenesis of *Arabidopsis thaliana*. Science 2003;301:653–7. [PubMed: 12893945]

Apuya NR, Yadegari R, Fischer RL, Harada JJ, Goldberg RB. *RASPBERRY3* gene encodes a novel protein important for embryo development. Plant Physiol 2002;129:691–705. [PubMed: 12068112]

Barton MK, Poethig RS. Formation of the shoot apical meristem in *Arabidopsis thaliana*: an analysis of development in the wild type and in the *shoot meristemless* mutant. Development 1993;119:823–831.

Beeckman T, Burssens S, Inzé D. The peri-cell-cycle in *Arabidopsis*. J Exp Bot 2001;52:403–11. [PubMed: 11326046]

Bennett SRM, Alvarez J, Bossinger G, Smyth DR. Morphogenesis in *pinoid* mutants of *Arabidopsis thaliana*. Plant J 1995;8:505–520.

Berleth T, Jürgens G. The role of the *monopteros* gene in organising the basal body region of the *Arabidopsis* embryo. Development 1993;118:575–587.

Blilou I, Frugier F, Folmer S, Serralbo O, Willemsen V, Wolkenfelt H, Eloy NB, Ferreira PC, Weisbeek P, Scheres B. The Arabidopsis *HOBBIT* gene encodes a CDC27 homolog that links the plant cell cycle to progression of cell differentiation. Genes Dev 2002;16:2566–75. [PubMed: 12368267]

Briggs GC, Osmont KS, Shindo C, Sibout R, Hardtke CS. Unequal genetic redundancies in *Arabidopsis*--a neglected phenomenon? Trends Plant Sci 2006;11:492–8. [PubMed: 16949326]

Camilleri C, Azimzadeh J, Pastuglia M, Bellini C, Grandjean O, Bouchez D. The Arabidopsis *TONNEAU2* gene encodes a putative novel protein phosphatase 2A regulatory subunit essential for the control of the cortical cytoskeleton. Plant Cell 2002;14:833–45. [PubMed: 11971138]

Chandler JW, Cole M, Flier A, Grewe B, Werr W. The AP2 transcription factors DORNRÖSCHEN and DORNRÖSCHEN-LIKE redundantly control *Arabidopsis* embryo patterning via interaction with PHAVOLUTA. Development. 2007

Di Laurenzio L, Wysocka-Diller J, Malamy JE, Pysh L, Helariutta Y, Freshour G, Hahn MG, Feldmann KA, Benfey PN. The *SCARECROW* gene regulates an asymmetric cell division that is essential for generating the radial organization of the Arabidopsis root. Cell 1996;86:423–33. [PubMed: 8756724]

Dolezel J, Gohde W. Sex determination in dioecious plants *Melandrium album* and *M. rubrum* using high-resolution flow cytometry. Cytometry 1995;19:103–6. [PubMed: 7743889]

Friml J, Vieten A, Sauer M, Weijers D, Schwarz H, Hamann T, Offringa R, Jürgens G. Efflux-dependent auxin gradients establish the apical-basal axis of Arabidopsis. Nature 2003;426:147–53. [PubMed: 14614497]

Haecker A, Gross-Hardt R, Geiges B, Sarkar A, Breuninger H, Herrmann M, Laux T. Expression dynamics of *WOX* genes mark cell fate decisions during early embryonic patterning in *Arabidopsis thaliana*. Development 2004;131:657–68. [PubMed: 14711878]

Hamann T, Mayer U, Jürgens G. The auxin-insensitive *bodenlos* mutation affects primary root formation and apical-basal patterning in the *Arabidopsis* embryo. Development 1999;126:1387–95. [PubMed: 10068632]

Hemerly AS, Ferreira P, de Almeida Engler J, Van Montagu M, Engler G, Inzé D. *cdc2a* expression in Arabidopsis is linked with competence for cell division. Plant Cell 1993;5:1711–23. [PubMed: 8305869]

Inzé D, De Veylder L. Cell cycle regulation in plant development. Annu Rev Genet 2006;40:77–105. [PubMed: 17094738]

Jenik PD, Barton MK. Surge and destroy: the role of auxin in plant embryogenesis. Development 2005;132:3577–85. [PubMed: 16077088]

Joubes J, Chevalier C, Dudits D, Heberle-Bors E, Inze D, Umeda M, Renaudin JP. CDK-related protein kinases in plants. Plant Mol Biol 2000;43:607–20. [PubMed: 11089864]

Jürgens G. Growing up green: cellular basis of plant development. Mech Dev 2003;120:1395–406. [PubMed: 14623445]

Laux T, Mayer KFX, Berger J, Jürgens G. The *WUSCHEL* gene is required for shoot and floral meristem integrity in *Arabidopsis*. Development 1996;122:87–96. [PubMed: 8565856]

Laux T, Wurschum T, Breuninger H. Genetic regulation of embryonic pattern formation. Plant Cell 2004;16 Suppl:S190–202. [PubMed: 15100395]

Long JA, Ohno C, Smith ZR, Meyerowitz EM. *TOPLESS* regulates apical embryonic fate in *Arabidopsis*. Science 2006;312:1520–3. [PubMed: 16763149]

Long JA, Woody S, Poethig S, Meyerowitz EM, Barton MK. Transformation of shoots into roots in *Arabidopsis* embryos mutant at the *TOPLESS* locus. Development 2002;129:2797–806. [PubMed: 12050130]

Lukowitz W, Roeder A, Parmenter D, Somerville C. A MAPKK kinase gene regulates extra-embryonic cell fate in *Arabidopsis*. Cell 2004;116:109–19. [PubMed: 14718171]

Mansfield SG, Briarty LG. Early embryogenesis in *Arabidopsis thaliana*. II. The developing embryo. Can J Bot 1991;69:461–76.

Martinez MC, Jørgensen JE, Lawton MA, Lamb CJ, Doerner PW. Spatial pattern of *cdc2* expression in relation to meristem activity and cell proliferation during plant development. Proc Natl Acad Sci USA 1992;89:7360–4. [PubMed: 1502145]

Masubelele NH, Dewitte W, Menges M, Maughan S, Collins C, Huntley R, Nieuwland J, Scofield S, Murray JA. D-type cyclins activate division in the root apex to promote seed germination in *Arabidopsis*. Proc Natl Acad Sci USA 2005;102:15694–9. [PubMed: 16227434]

Mayer U, Torres Ruiz RA, Berleth T, Miséra S, Jürgens G. Mutations affecting body organization in the *Arabidopsis* embryo. Nature 1991;353:402–407.

Park SO, Zheng Z, Oppenheimer DG, Hauser BA. The *PRETTY FEW SEEDS2* gene encodes an *Arabidopsis* homeodomain protein that regulates ovule development. Development 2005;132:841–9. [PubMed: 15659481]

Prigge MJ, Otsuga D, Alonso JM, Ecker JR, Drews GN, Clark SE. Class III homeodomain-leucine zipper gene family members have overlapping, antagonistic, and distinct roles in Arabidopsis development. Plant Cell 2005;17:61–76. [PubMed: 15598805]

Sarkar AK, Luijten M, Miyashima S, Lenhard M, Hashimoto T, Nakajima K, Scheres B, Heidstra R, Laux T. Conserved factors regulate signalling in *Arabidopsis thaliana* shoot and root stem cell organizers. Nature 2007;446:811–4. [PubMed: 17429400]

Sessions A, Weigel D, Yanofsky MF. The *Arabidopsis thaliana MERISTEM LAYER 1* promoter specifies epidermal expression in meristems and young primordia. Plant J 1999;20:259–63. [PubMed: 10571886]

Shevell D, Leu WM, Gilmour CS, Xia G, Feldmann KA, Chua NH. *EMB30* is essential for normal cell division, cell expansion, and cell adhesion in Arabidopsis and encodes a protein that has similarity to Sec7. Cell 1994;77:1051–1062. [PubMed: 8020095]

Steinmann T, Geldner N, Grebe M, Mangold S, Jackson CL, Paris S, Galweiler L, Palme K, Jürgens G. Coordinated polar localization of auxin efflux carrier PIN1 by GNOM ARF GEF. Science 1999;286:316–8. [PubMed: 10514379]

Till BJ, Reynolds SH, Greene EA, Codomo CA, Enns LC, Johnson JE, Burtner C, Odden AR, Young K, Taylor NE, Henikoff JG, Comai L, Henikoff S. Large-scale discovery of induced point mutations with high-throughput TILLING. Genome Res 2003;13:524–30. [PubMed: 12618384]

Torres-Ruiz RA, Jürgens G. Mutations in the *FASS* gene uncouple pattern formation and morphogenesis in *Arabidopsis* development. Development 1994;120:2967–78. [PubMed: 10484674]

Vroemen CW, Mordhorst AP, Albrecht C, Kwaaitaal MA, de Vries SC. The *CUP-SHAPED COTYLEDON3* gene is required for boundary and shoot meristem formation in *Arabidopsis*. Plant Cell 2003;15:1563–77. [PubMed: 12837947]

Weigel, D.; Glazebrook, J. *Arabidopsis*: A Laboratory Manual. Cold Spring Harbor Laboratory Press; Cold Spring Harbor, NY: 2002.

Weijers D, Jürgens G. Auxin and embryo axis formation: the ends in sight? Curr Opin Plant Biol 2005;8:32–7. [PubMed: 15653397]

Willemsen V, Scheres B. Mechanisms of pattern formation in plant embryogenesis. Annu Rev Genet 2004;38:587–614. [PubMed: 15568987]

Willemsen V, Wolkenfelt H, de Vrieze G, Weisbeek P, Scheres B. The *HOBBIT* gene is required for formation of the root meristem in the *Arabidopsis* embryo. Development 1998;125:521–31. [PubMed: 9425146]

Wu X, Dabi T, Weigel D. Requirement of homeobox gene *STIMPY/WOX9* for *Arabidopsis* meristem growth and maintenance. Curr Biol 2005;15:436–40. [PubMed: 15753038]

Wu X, Dinneny JR, Crawford KM, Rhee Y, Citovsky V, Zambryski PC, Weigel D. Modes of intercellular transcription factor movement in the Arabidopsis apex. Development 2003;130:3735–45. [PubMed: 12835390]

Yadegari R, Paiva G, Laux T, Koltunow AM, Apuya N, Zimmerman JL, Fischer RL, Harada JJ, Goldberg RB. Cell differentiation and morphogenesis are uncoupled in Arabidopsis *raspberry* embryos. Plant Cell 1994;6:1713–1729. [PubMed: 12244232]

Zhu J, Shi H, Lee BH, Damsz B, Cheng S, Stirm V, Zhu JK, Hasegawa PM, Bressan RA. An *Arabidopsis* homeodomain transcription factor gene, HOS9, mediates cold tolerance through a CBF-independent pathway. Proc Natl Acad Sci USA 2004;101:9873–8. [PubMed: 15205481]

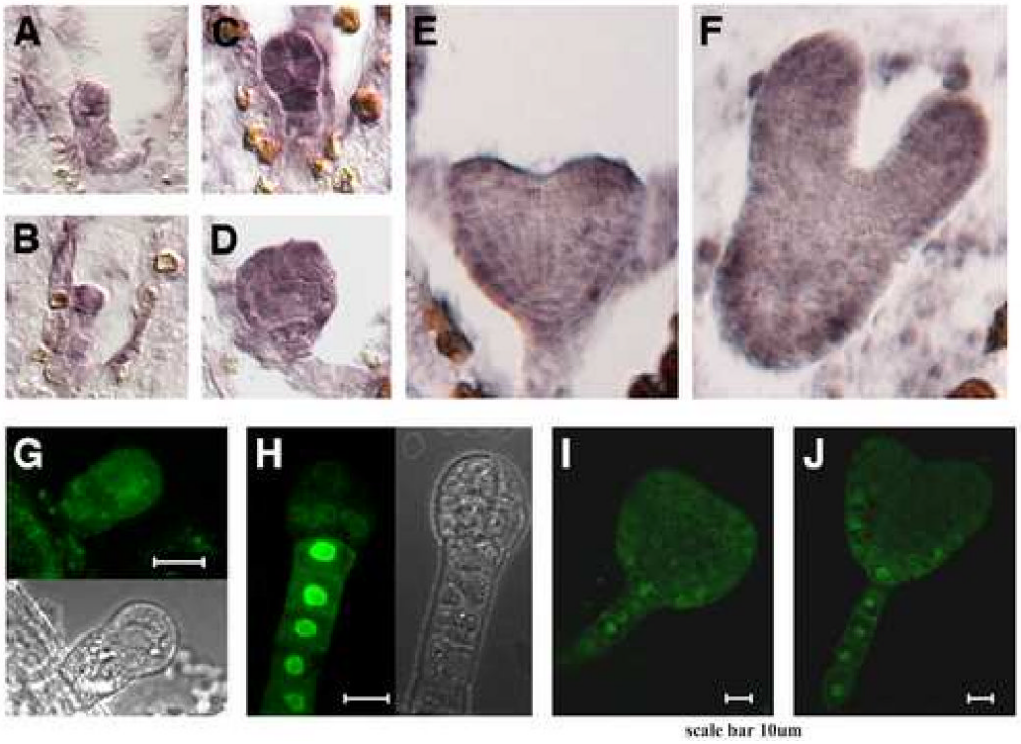

Figure 1. *STIP* expression in developing embryos

(A-F)*STIP* mRNA detected by *in situ* hybridization using an anti-sense *STIP* probe in (A) zygote after the first division, (B) one-cell, (C) octant, (D) globular, (E) heart, and (F) torpedo stage embryos.

(G-J) STIP:GFP fusion protein expression in rescued *stip*-2 plants, in (G) zygote after the first division, (H) globular, (I) transition, and (J) heart stage embryos. For better visualization, maximum projections of optical section series are shown in (G) and (H), corresponding DIC images are also shown in the same panels. (I) and (J) are images from single optical sections. Scale bar represents 10 μm.

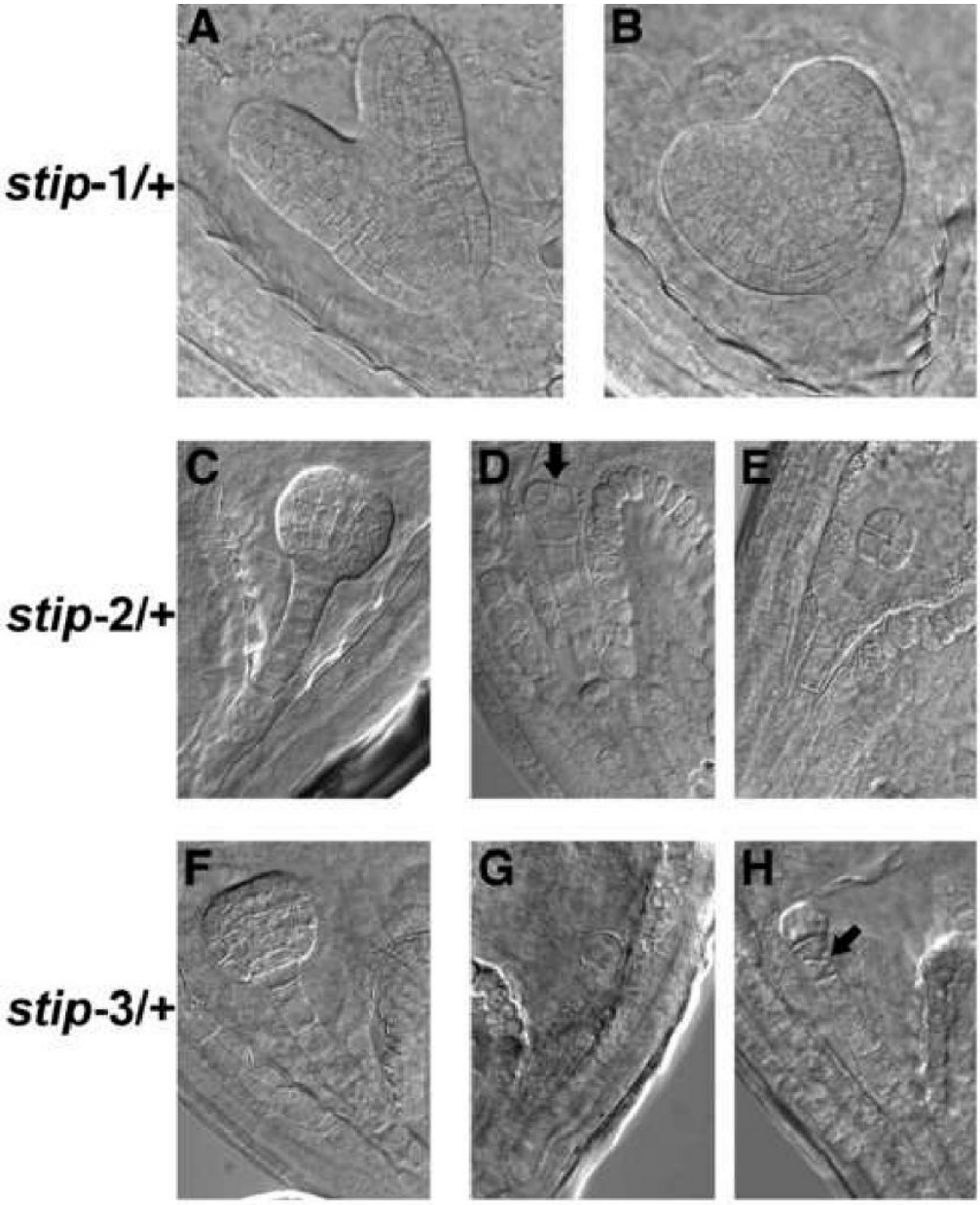

Figure 2. The embryonic phenotype of different *stip* alleles

(A-B) Torpedo stage normal (A) and *stip*-1 (B) embryos from a *stip*-1/+ plant. *stip*-1 embryos show reduced apical-basal growth and lateral cell expansion.

(C-E) Globular stage normal (C) and *stip*-2 (D, E) embryos from a *stip*-2/+ plant. *stip*-2 embryos can have cell division defect as early as the first division (D, arrow), and most arrest growth by octant stage (E).

(F-H) Globular stage normal (F) and *stip*-3 (G, H) embryos from a *stip*-3/+ plant. *stip*-3 embryos arrest within the first one or two divisions, some also having cell division defects in the suspensor region (arrow in H).

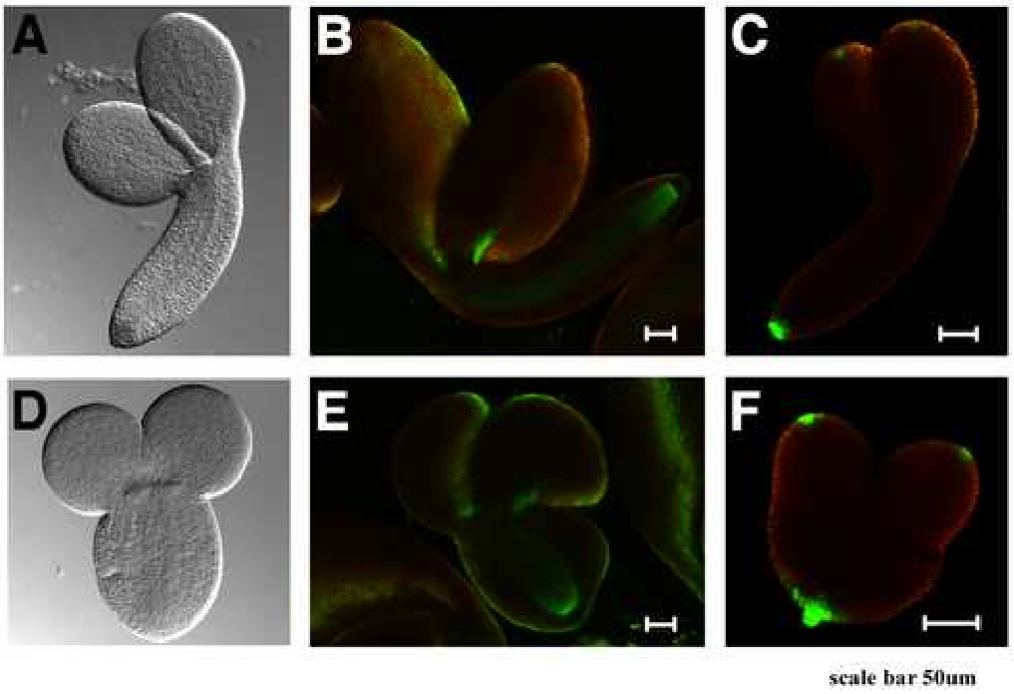

Figure 3. SCR::GFP and DR5rev::GFP expression in wild-type and *stip*-1 embryos

(A, D) DIC images of a mature wild-type embryo (A) and a *stip*-1 embryo of intermediate phenotype (D).

(B, E) SCR::GFP expression in wild-type (B) and *stip*-1 (E) embryos. (C, F) DR5rev::GFP expression in wild-type (C) and *stip*-1 (F) embryos. GFP fluorescence is in green, and auto-fluorescence is in red. Both markers show normal localization and expression levels in the mutant embryos. Scale bar represents 50 μm.

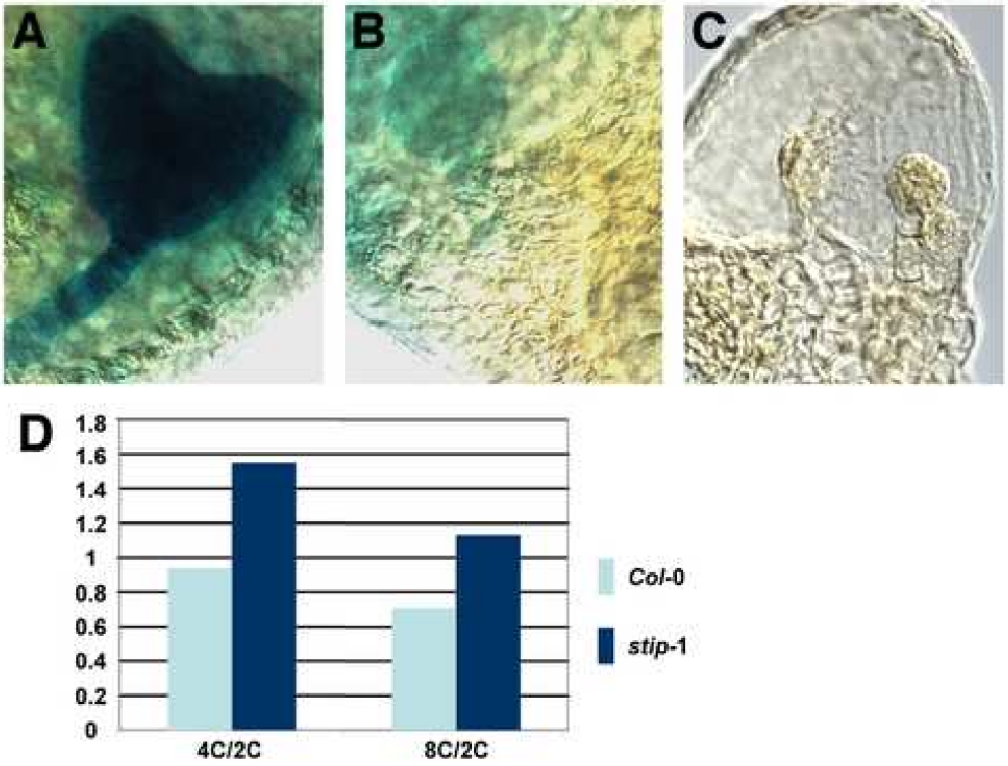

Figure 4. *stip* embryos show cell cycle arrest

(A-C) CDKA;1:: GUS activity in normal (A) and *stip*-2 (B, C) embryos derived from a *stip*-2/+; CDKA;1::GUS plant. *stip*-2 embryos have either much reduced (B) or no (C) GUS staining.

(D) Ratios between nuclei of different ploidy from wild-type and *stip*-1 roots. The *stip*-1 sample has a significantly higher ratio of tetraploid (4C) or octaploid (8C) nuclei to diploid (2C) nuclei.

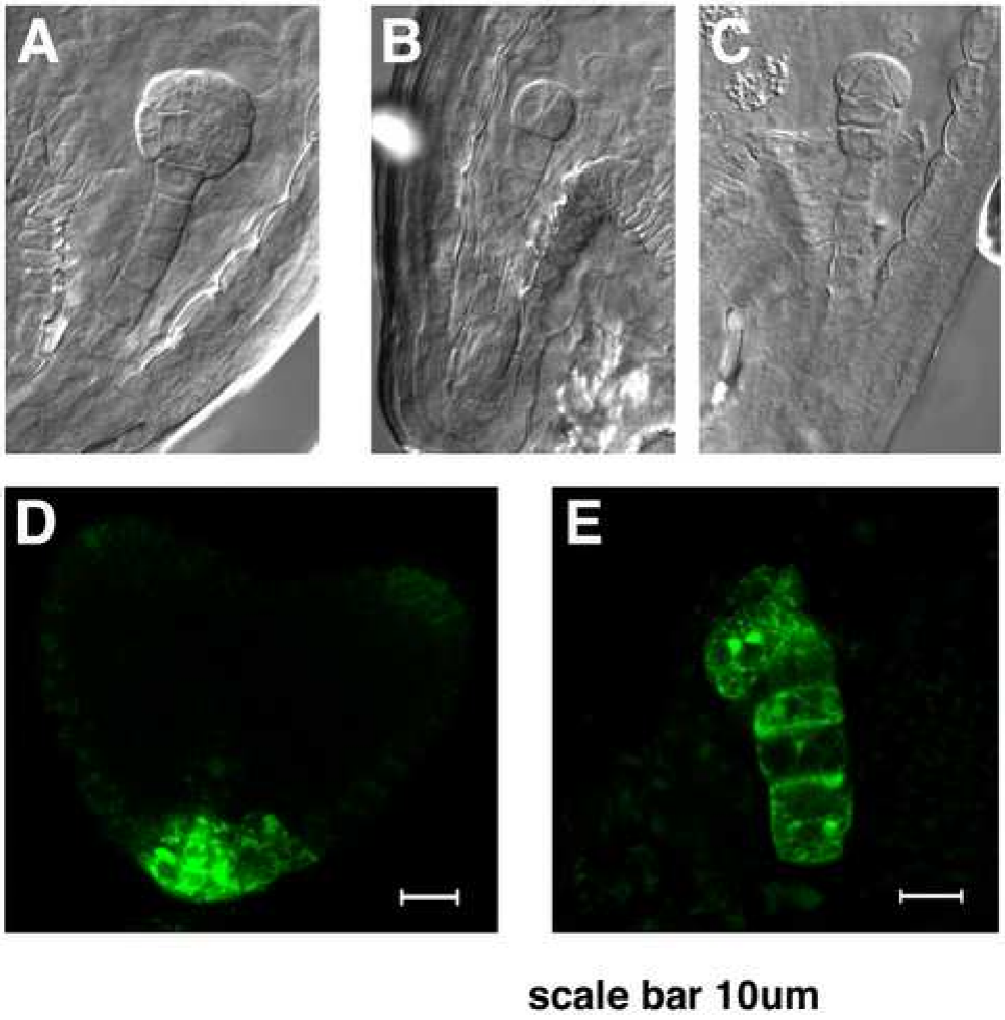

Figure 5. Embryonic phenotype of putative *stip*-1 *stpl*-1 double mutants

(A-C) Globular stage normal (A) and putative *stip*-1 *stpl*-1 (B, C) embryos from a *stpl*-1/*stpl*-1 *stip*-1/+ plant. The double mutant embryos show defects as early as the first cell division, and arrest growth soon after.

(D-E) DR5rev::GFP expression in heart stage normal (D) and putative *stip*-1 *stpl*-1 (E) embryos. GFP fluorescence is seen in both the embryo proper and the suspensor of the arrested double mutant embryo (E). Scale bar represents 10 μm.

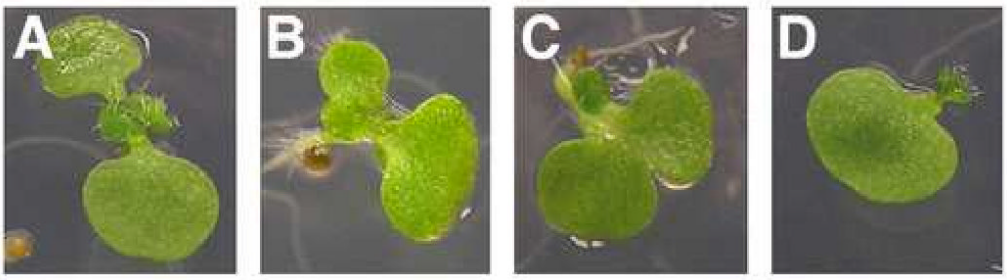

Figure 6. Variable seedling phenotype of *stpl*-1 *wox2*

7-day-old *stpl*-1 *wox2* double mutant seedlings can have two normal cotyledons similar to wild type (A), unequal cotyledons (B), heart-shaped (C), and single (D) cotyledons. The first pair of true leaves is also affected in (B-D).

Table 1

stip and *stpl* phenotype at the time of seed maturity.

parental genotype	total embryos	normal	reduced size	arrested before globular stage
stip-1/+	116	76	37 (31.9%)	3 (2.6%)
stip-2/+	171	118	7 (4.1%)	46 (26.9%)
stip-3/+	143	91	13 (9.1%)	39 (27.3%)
stip-1/+; *stpl*-1/*stpl*-1	122	102	1 (0.8%)	19 (15.6%) *

* Some early embryonic death caused ovules to abort, so this portion may be under-represented.

Table 2

STIP expression levels in different genotypes.

genotype	Col/-0	stip-1	stpl/-1
tissue			
Inflorescences	6.68	0.00056	7.46
open flowers	1.82	0.00065	2.47
green siliques	2.06	0.00047	2.20

Note: Levels are relative to reference transcript At5g15400, which remained constant in all samples.

Table 3

Distribution of nuclei in different cell cycle stages.

genotype	total nuclei	2C	S phase	4C	total nuclei	4C	S phase	8C
wild type	9868	33.3%	29.5%	31.2%	8967	45.1%	20.9%	34.1%
stip-1	11521	29.2%	20.3%	45.4%	12031	49.7%	13.8%	36.1%

Note: A chi-square test shows that the distribution of nuclei in the different fractions are statistically significantly different between the two genotypes with p-values much smaller than 0.001.